Complex dynamics in one-dimensional CNNs

István Petrás and Marco Gilli

Analogic and Neural Computing Systems Laboratory
Computer and Automation Research Institute of the Hungarian Academy of Sciences,
Kende u.11, Budapest, 1111 – Hungary

Department of Electronics, Politecnico di Torino
Corso Duca degli Abruzzi 24, I-10129 Torino, Italy

petras@sztaki.hu, marco.gilli@polito.it

Abstract. The effect of boundary conditions on the global dynamics of cellular neural networks (CNNs) is investigated. As a case study one-dimensional template CNNs are considered. It is shown that if the off-diagonal template elements have opposite sign, then the boundary conditions behave as bifurcation parameters and can give rise to a very rich and complex dynamic behavior. In particular they determine the equilibrium point patterns, the transition from stability to instability and the occurrence of several bifurcation phenomena leading to strange and/or chaotic attractors and to the coexistence of several attractors. Then the influence of the number of cells on the global dynamics is studied, with particular reference to the occurrence of hyperchaotic behavior.

1. Introduction

As far as the dynamic behavior is concerned, cellular neural networks (CNNs) can be divided in two main classes: stable CNNs, in which each trajectory (with at most the exception of a set of measure zero) converges to an equilibrium point and unstable CNNs which possess at least one attractor that is not a stable equilibrium point. Stable CNNs have been mainly exploited in image processing applications, that require the convergence to a stationary equilibrium point. CNN stability has been studied in several papers. Complete stability (i.e. convergence to a constant equilibrium point from each initial condition) was proved for symmetric templates in [1] and [2], for acyclic templates in [3] and for a class of non-symmetric templates in [4,5]. Stability almost everywhere was proved for positive cell linking templates in [6] and for a class of sign-symmetric templates in [2]. CNNs described by one-dimensional (1D) opposite sign template were investigated in [7] and [8] where some conditions for complete stability were given. In [9, 10] the global dynamic behavior of 1D template CNNs was studied by introducing the useful concepts of *local diffusion* [9] and *global propagation* [10]. In addition some theorems on the number of stable equilibrium points were proved in [9].

The class of unstable CNNs received less attention. Oscillating behavior was firstly investigated in opposite sign template CNNs [6, 7]. Further examples of CNNs exhibiting limit cycles were shown in [10] – [23]. Non-periodic complex dynamic behavior has been observed in different CNN models: I) non-autonomous two-cell systems [24]; II) autonomous three cell CNNs described by space-variant templates [12]; III) autonomous fully connected three cell networks [23]; IV) delayed CNNs [25]; V) state controlled CNNs [14]; VI) autonomous space-invariant CNNs, composed by at least 3 x 3 cells [11, 13]; VII) 1D and 2D CNNs, with constant external inputs [26].

2. Effect of boundary conditions

Most of the theoretical investigations on CNN dynamics, with the exception of some general stability results, focused on the influence of template parameters. In [27] it was shown that spatial boundary conditions have a significant impact on CNN dynamics. In particular there exists a subclass of CNNs, whose stability depends on the boundary conditions. In [27] the author presented an example of a CNN with opposite sign template of the form [s p –s] that is stable if the boundary conditions are ±1 and unstable with zero boundary conditions.

On the other hand, it is known that 1D CNNs described by the opposite sign template [s p –s], with zero input and boundary conditions, do not possess stable equilibrium point if $0<p-1<s$ and hence are unstable.

In this manuscript we will investigate the effect of boundary conditions on the global dynamic behavior of CNNs. We will show that constant boundary conditions behave as bifurcation parameters and determine the equilibrium point patterns and the transition from stability to instability. They also characterize the type of instability, in particular the occurrence of periodic, quasi-periodic, non-periodic and/or chaotic behavior.

We consider 1D CNNs, described by either three (**A**= [s p r]) of five dimensional template (**A**=[w s p r v]). They can be modeled by the following simplified equation, where the input terms are incorporated into the parameter β.

$$\dot{x}_i = -x_i + wf(x_{i-2}) + sf(x_{i-1}) + pf(x_i) + rf(x_{i+1}) + vf(x_{i+2}) + \beta \qquad (1)$$

where f is a Lipschitz monotonic non linear function, that in most cases admits of the following piecewise linear expression:

$$f(x) = \tfrac{1}{2}\left(|x+1| - |x-1|\right)$$

For the sake of the completeness we here summarized the main results, concerning these networks.

Theorem 1 [28] If the template elements of equations (1) satisfy the constraints $wv \geq 0$ and $sr \geq 0$, then the corresponding CNN is completely stable (i.e. all trajectories converge towards an equilibrium point) for any external constant inputs and boundary conditions.

Proof : it is derived from Theorem 1 and Theorem 2 of [4].

Theorem 2 [10] Let N be the number of cells of a CNN, described by equation (1), with zero boundary conditions and inputs (i.e. $\beta=0$), with $w = v = 0$, and satisfying $p-1<|s-r|$, $p>1$. If $N \geq 3$, the number S(N) of stable equilibrium points admits of the following expression:

2N, if $\max\{|r|,|s|\} < p-1 < |s-r|$

2, if $\min\{|r|,|s|\} < p-1 < \max\{|r|,|s|\}$

2, if $p-1 < \max\{\min(r,s), \min(-r,-s)\}$

0, if $p-1 < \max\{\min(-r, s), \min(r, -s)\}$

Proof: See [10].

Theorem 3 [7] If $r = -s$, $\beta=0$ and $s>p-1>0$, then the CNN described by equation (1), with $w = v = 0$ has no stable equilibrium point.

Proof: See [7].

Theorem 4 [7] If $r = -s$, $\beta=0$ and $0 < s<(p-1)/2$, then the CNN described by equation (1) with $w = v = 0$ is completely stable.

Proof: See [7].

In order to analyze the effect of the boundary conditions, we will focus on 1D CNNs, described by equation (1) with $w = v = 0$, $p - 1>0$, and $r = -s$, i.e. by the template:

$$\mathbf{A}= [s\ p\ -s] \quad (p - 1 >0) \qquad (2)$$

Since $p - 1 > 0$, all stable equilibrium point are located in saturation regions (see [1]) and can be characterized by the output functions $y_i = f(x_i)$. For a N cell CNN, they are described by patterns of the type $\{y_1, y_2, \ldots, y_k, \ldots, y_{N-1}, y_N\}$, where y_i is either +1 or -1.

We will restrict our attention to the case $0 < p - 1 < s$, that, in case of zero boundary conditions, implies the absence of stable equilibrium points (see [7]).

In order to compute all possible stable patterns for a given CNN with arbitrary boundary conditions, the following Definitions and Propositions are useful. Hereafter the left and the right boundary conditions of a N-cell CNN will be denoted by X_0 and X_{N+1} respectively.

***Definition 1*:** A boundary pattern $\{y_1, y_2\}$ located on the left side of a 1D CNN composed by N cells and described by template (2), is said to be admissible if and only if:

$$[(p-1)\, y_1 + s\, X_o - s\, y_2]\, y_1 > 0 \qquad (3)$$

***Definition 2*:** A boundary pattern $\{y_{N-1}, y_N\}$ located on the right side of a 1D CNN composed by N cells and described by template (2), is said to be admissible if and only if:

$$[(p-1)\, y_N - s\, X_{N+1} + s\, y_{N-1}]\, y_N > 0 \qquad (4)$$

***Definition 3*:** A central pattern $\{y_{i-1}, y_i, y_{i+1}\}$ of a 1D CNN composed by N cells and described by template (2), is said to be admissible if and only if:

$$[(p-1)\, y_i - s\, y_{i+1} + s\, y_{i-1}]\, y_i > 0 \qquad (5)$$

Definition 4: *A* 1D CNN composed by N cells, described by template (2), and with generic boundary conditions X_0 and X_{N+1} is associated to a directed graph G, which contains three kinds of nodes: the initial nodes $\mathcal{N}_i$ that are represented by all the admissible left boundary patterns, the central nodes $\mathcal{N}_c$, corresponding to all the admissible central patterns and the final nodes $\mathcal{N}_f$, i.e. all the admissible right boundary patterns.
The connections among the nodes are defined according to the following rules:

- an initial node $n_i=\{I_1,I_2,\}$ is directly connected to a central node $n_c=\{C_1,C_2,C_3,\}$ *if and only if* $I_1=C_1$ and $I_2=C_2$, where $I_i, C_i \in \{-1,1\}$.
- a central node $n^k_c = \{C^k_1, C^k_2, C^k_3,\}$ is directly connected to a central node $n_c^{k+1} = \{C_1^{k+1}, C_2^{k+1}, C_3^{k+1}\}$ *if and only if* $C^k_2 = C_1^{k+1}$ *and* $C^k_3 = C_2^{k+1}$ where C_i^k, $C_i^{k+1} \in \{-1,1\}$.
- a central node $n_c=\{C_1,C_2,C_3,\}$ is directly connected to a final node $n_f=\{F_1, F_2,\}$ *if and only if* $C_2=F_1$ *and* $C_3=F_2$, where $C_i, F_i \in \{-1,1\}$.

The graph defined above allows one to characterize the equilibrium point patterns according to the following Proposition:

Proposition: *A* 1D CNN composed by N cells, described by template (2), and with generic boundary conditions X_0 and X_{N+1} admits of an equilibrium point if and only if the graph associated to the network exhibits a path of length N connecting an initial node $n_i=\{I_1,I_2,\}$ to a final node $n_f=\{F_1, F_2,\}$, through a sequence of central nodes $n^k_c = \{C^k_1, C^k_2, C^k_3,\}$ $(2 \le k \le N-1)$. If such a path exists, the corresponding equilibrium point is described by the following pattern $\{y_1, y_2, \ldots, y_k, \ldots, y_{N-1}, y_N\} = \{I_1, C^2_2, \ldots, C^k_2, \ldots, C^{N-1}_2, F_2\}$.

Proof: It is readily derived by noting that, according to Definitions 1-3, a sequence of admissible patterns, gives rise to a stable equilibrium point.

Fig. 1 shows the associated graph, in case of zero boundary conditions ($X_0 = X_{N+1} = 0$), for $s > p - 1 > 0$. It is seen that there exists no path connecting initial and final nodes, which is in agreement with the fact that the network does not exhibit stable equilibrium points (see [7]).

Fig. 2 shows another set of boundary conditions ($|X_{N+1}|<1-(p-1)/s$, $|X_0+1|<(p-1)/s$); the corresponding admissible path is represented in bold and, according to the Proposition above, gives rise to an equilibrium point pattern of the type {-1, -1, …, -1, …, -1, -1}.

Table 1 reports the possible equilibrium point patterns, as a function of the left and of the right boundary conditions, X_0 and X_{N+1}. They have been derived by constructing the corresponding associate graph for each set of significant boundary conditions. Such patterns can be described as strings of {+1,–1}, that are expressed, according to the following notations: a) the string $\{a, b\}^0$ represents the null string; b) the expression $\{a, b\}^n$ denotes a string obtained by repeating n times the symbols a and b, e.g. $\{a, b\}^3 = a, b, a, b, a, b$.

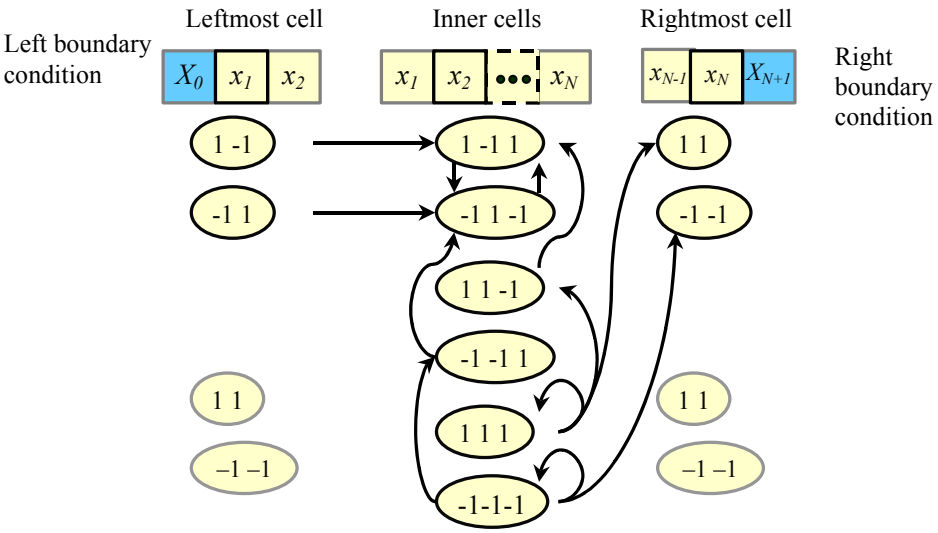

Figure 1. Graph associated to the network, in case of zero boundary conditions ($X_0=0$, $X_{N+1}=0$) and p-1<s. There is no path connecting initial and final nodes, which implies the absence of stable equilibrium points.

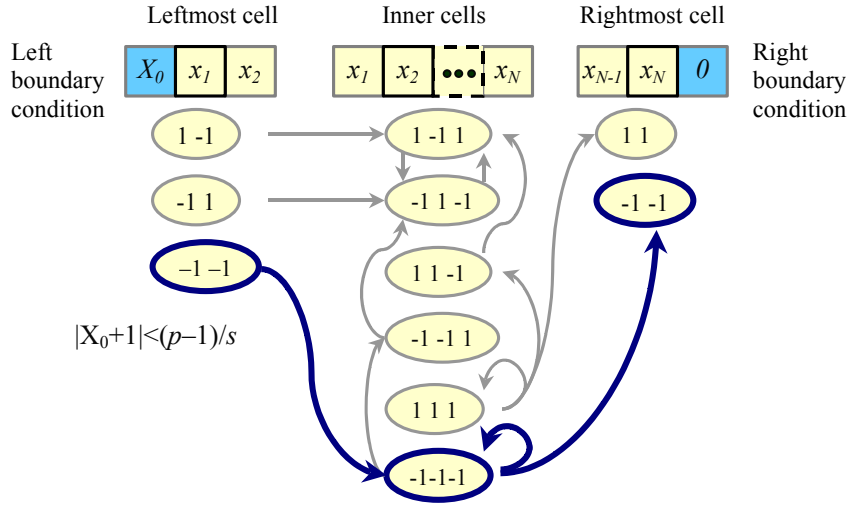

Figure 2. Graph associated to the network for {$|X_{N+1}|<1-(p-1)/s$, $|X_0+1|<(p-1)/s$} and p-1<s. The only path connecting an initial and a final node is represented in bold. This gives rise to an equilibrium point of the type {-1, -1, …, -1, -1}.

Table 1 shows that the set of boundary conditions satisfying {$|X_0|<1–(p–1)/s$, $|X_{N+1}|<1–(p–1)/s$} implies the absence of stable equilibrium points. It is therefore expected that in this parameter region the network is unstable and complex dynamics may occur. For all the other sets of boundary conditions the network exhibits at least one stable equilibrium point. As we will show later, this does not exclude the existence of periodic or complex dynamic behavior.

Equilibrium point patterns	$X_{N+1} < \frac{-(p-1+s)}{s}$	$\lvert X_{N+1}+1\rvert < \frac{p-1}{s}$	$\lvert X_{N+1}\rvert < \frac{-(p-1)+s}{s}$	$\lvert X_{N+1}-1\rvert < \frac{p-1}{s}$	$X_{N+1} > \frac{p-1+s}{s}$
$X_0 < \frac{-(p-1+s)}{s}$	$-1,\{-1\}^n,+1,-1,\{+1,-1\}^m,+1$ $-1,\{-1\}^n,+1$	$-1,\{-1\}^n,+1,-1,\{+1,-1\}^m,+1$ $-1,\{-1\}^n,+1$ $-1,\{-1\}^n,-1$	$-1,\{-1\}^n,-1$	$-1,\{-1\}^n,+1,\{-1,+1\}^m,-1$ $-1,\{-1\}^n,-1$	$-1,\{-1\}^n,+1,\{-1,+1\}^m,-1$ $-1,\{-1\}^n,-1$
$\lvert X_0+1\rvert < \frac{p-1}{s}$	$-1,\{-1\}^n,+1,-1,\{+1,-1\}^m,+1$ $+1,-1,\{+1,-1\}^n,+1$ $-1,\{-1\}^n,+1$	$-1,\{-1\}^n,+1,\{-1,+1\}^m,-1$ $+1,-1,+1,\{-1,+1\}^n,-1$ $-1,\{-1\}^n,-1$	$-1,\{-1\}^n,-1$	$+1,-1,+1,\{-1,+1\}^m,-1$ $-1,+1,\{-1,+1\}^n,-1$	$+1,-1,+1,\{-1,+1\}^n,-1$ $-1,+1,\{-1,+1\}^n,-1$
$\lvert X_0\rvert < \frac{-(p-1)+s}{s}$	$-1,+1,-1,\{+1,-1\}^n,+1$ $+1,-1,\{+1,-1\}^n,+1$	$-1,+1,-1,\{+1,-1\}^n,+1$ $+1,-1,\{+1,-1\}^n,+1$	*No equilibrium points*	$-1,-1,+1,\{-1,+1\}^n,-1$ $-1,\{-1\}^n,-1$	$-1,\{-1\}^n,+1,\{-1,+1\}^m,-1$ $-1,\{-1\}^m,-1$
$\lvert X_0-1\rvert < \frac{p-1}{s}$	$+1,\{+1\}^n,-1,\{+1,-1\}^m,+1$ $-1,+1,-1,\{+1,-1\}^n,+1$ $+1,\{+1\}^n,+1$	$+1,\{+1\}^n,-1,\{+1,-1\}^m,+1$ $-1,+1,-1,\{+1,-1\}^n,+1$ $+1,\{+1\}^n,+1$	$+1,\{+1\}^n,+1$	$+1,\{+1\}^n,-1,+1,\{-1,+1\}^m,-1$ $-1,+1,\{-1,+1\}^n,-1$ $+1,\{+1\}^n,-1$ $+1,\{+1\}^n,+1$	$+1,\{+1\}^n,-1,+1,\{-1,+1\}^m,-1$ $-1,+1,\{-1,+1\}^n,-1$ $+1,\{+1\}^n,-1$
$X_0 > \frac{p-1+s}{s}$	$+1,\{+1\}^n,-1,\{+1,-1\}^m,+1$ $+1,\{+1\}^n,+1$	$+1,\{+1\}^n,-1,\{+1,-1\}^m,+1$ $+1,\{+1\}^n,+1$	$+1,\{+1\}^n,+1$	$+1,\{+1\}^n,-1,+1,\{-1,+1\}^m,-1$ $+1,\{+1\}^n,-1$ $+1,\{+1\}^n,+1$	$+1,\{+1\}^n,-1,+1,\{-1,+1\}^m,-1$ $+1,\{+1\}^n,-1$

Table 1. The Table reports a compact expression for all the possible stable equilibrium point patterns in a CNN composed by *N* cells and described by a 1D template [s, p, -s] (p - 1 < s and s > 0) with boundary conditions X_0 and X_{N+1} . The two parameters n and m denote nonnegative integer numbers. The string expression $\{a, b\}^0$ represent the null string, whereas the expression $\{a, b\}^n$ denotes a string obtained by repeating n times the symbols a and b, e.g. $\{a, b\}^3$ = *a*, *b*, *a*, *b*, *a*, *b*.

3. Complex dynamic behavior in 1D CNNs

In this section we will show that constant boundary conditions may give rise to a complex dynamics, including the occurrence of several bifurcation processes leading to strange and/or chaotic behavior and to the coexistence of non-stationary attractors. The analysis is based on the theoretical results of the previous section and is mainly carried out through numerical simulation and via the computation of the Lyapunov exponents.

3.1 Periodic, quasi-periodic and chaotic behavior in 1D CNNs

We consider a 1D CNN, described by the antisymmetric template (2) with p = 1.1, and s = -r = 0.9,

$$\mathbf{A=[\ 0.9 \quad 1.1 \quad -0.9\ ]} \qquad (6)$$

We also assume that the input β is null and that function $f(x)$ can be approximated through a C^1 function $f_\varepsilon(x)$, that admits of a continuous first order derivative and that is equivalent to the original piecewise linear function when the parameter ε tends to zero [11].

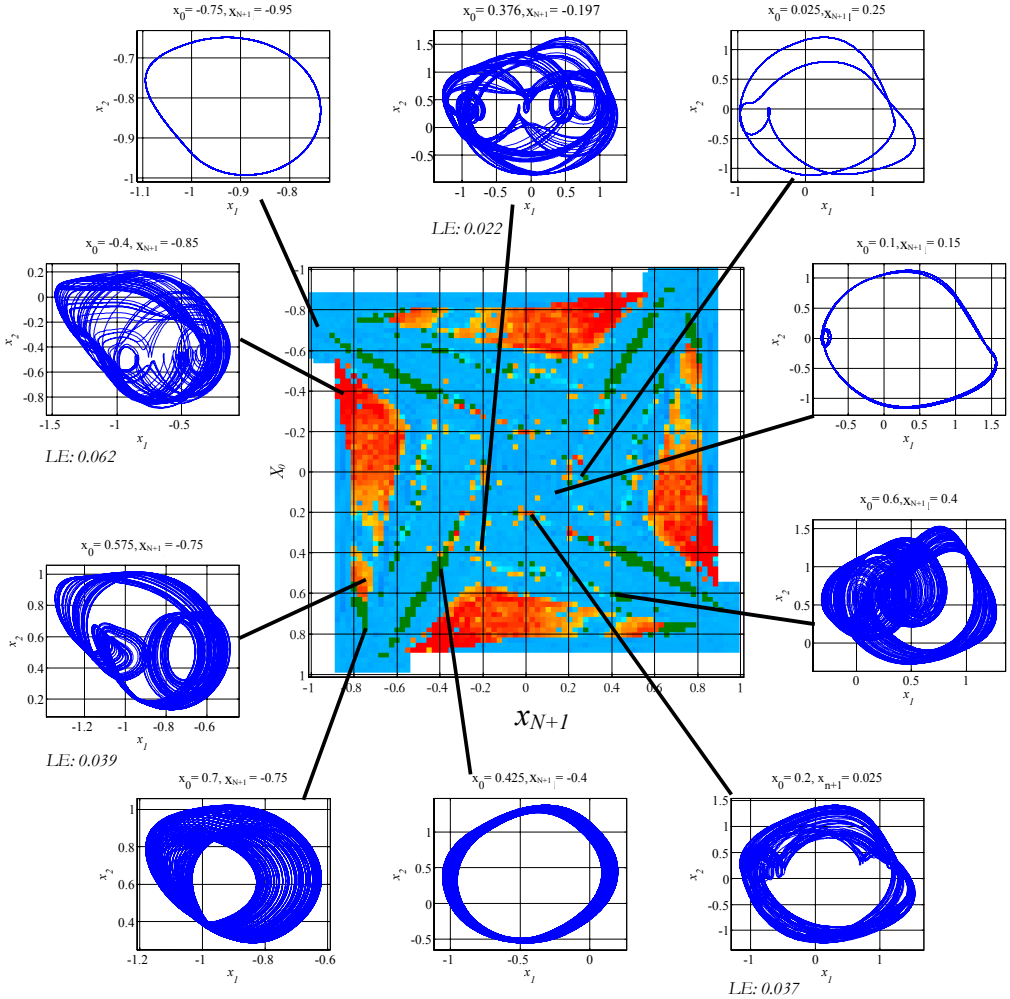

Figure 3. Dynamic behavior and Lyapunov exponents in a 4-cell CNN, described by a template A=[0.9 1.1 -0.9]. Horizontal – vertical axes: boundary conditions (X_0, X_{N+1}). Some attractors are shown. Color code: Yellow-red: chaotic attractor; green: torus (quasi-periodic behavior); blue: limit cycle (periodic behavior); white: equilibrium point (stable behavior). Initial conditions are assumed to be zero for all cells.

$$f_\varepsilon(x)=\begin{cases} -1 & x \le -(1+\varepsilon) \\ \frac{1}{4\varepsilon}\left[x^2+2(1+\varepsilon)x+(1-\varepsilon)^2\right] & |x+1| \le \varepsilon \\ x & |x| \le 1-\varepsilon \\ -\frac{1}{4\varepsilon}\left[x^2-2(1+\varepsilon)x+(1-\varepsilon)^2\right] & |x-1| \le \varepsilon \\ 1 & x \ge 1+\varepsilon \end{cases}$$

Fig. 3 reports the Lyapunov exponents in the boundary condition parameter space (X_0 , X_{N+1}) for a CNN composed by 4 cells. It is seen that the parameter space is divided in three main regions, corresponding to periodic behavior (blue area with one zero Lyapunov exponent), quasi periodic behavior (green area, with two zero Lyapunov exponents) and chaotic behavior (red area, with one positive Lyapunov exponents). The exponents have been computed by exploiting the algorithm described in [29] and the Lyapunov exponent toolbox (LET) for MATLAB developed by S. W. Kam. Fig. 3 also shows the projection onto a 2D plane of some characteristic attractors (periodic, quasi-periodic, chaotic) for a 4 cell CNN, described by template (6).

Fig. 4 shows a bifurcation diagram obtained by selecting in Fig. 3, a left boundary condition X_0 equal to 0.66 and by varying the right boundary condition X_{N+1} in the interval [-0.78…0.2]. Fig. 5 shows the period doubling bifurcation, occurring in Fig. 4, for a boundary condition X_{N+1} lying in the range [-0.3665…-0.361]. Fig. 6a presents the corresponding 2D projected trajectories.

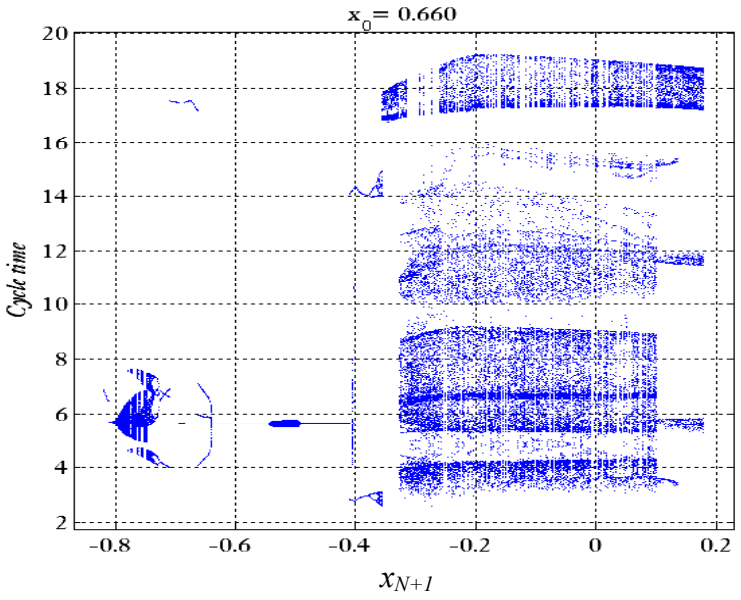

Figure 4. CNN composed by 4 cells and described by the template A=[0.9 1.1 -0.9]. Bifurcation diagram obtained by fixing the left boundary condition X_0 to 0.66 and varying the right boundary condition X_{N+1} in the interval [-0.78 0.2]. Initial conditions are assumed to be zero for all cells

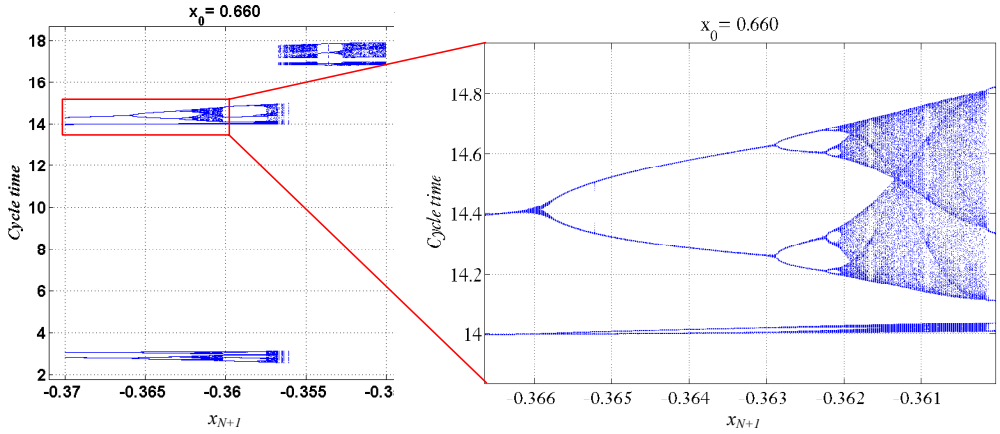

Figure 5. CNN composed by 4 cells and described by the template A=[0.9 1.1 -0.9]. Zoomed representation of the period doubling bifurcation, occurring in Fig. 5 for X_{N+1} lying in the range [-0.3665…-0.361]. Initial conditions are assumed to be zero for all cells.

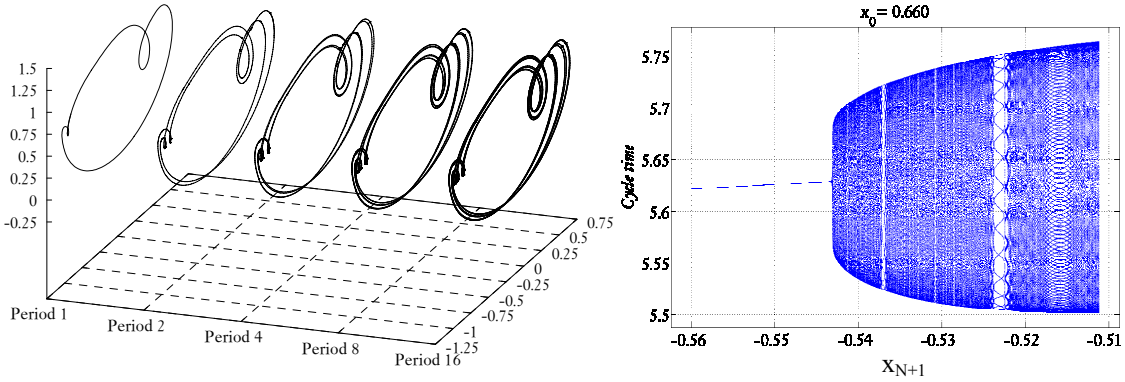

Figure 6. a) CNN composed by 4 cells and described by the template A=[0.9 1.1 -0.9]. Period doubling bifurcation occurring at $\{X_0; X_{N+1}\}=\{0.66, -0.3665 \ldots -0.361\}$ and corresponding trajectories. Initial conditions are assumed to be zero for all cells. b) Naimark-Sacker bifurcation. $\{X_0; X_{n+1}\}=\{0.66, -0.56 \ldots -0.51\}$; A=[–0.9 1.10 0.9]; Dimension: 4×1. Initial condition is zero for all cell.

Fig. 6b focuses on the transition from quasi-periodic to periodic behavior occurring at $X_{N+1}=\{-0.56\ldots-0.51\}$, through a Naimark-Sacker bifurcation. It is worth observing the presence of periodic windows in the quasi-periodic region. The corresponding trajectories are shown in Fig. 7a.

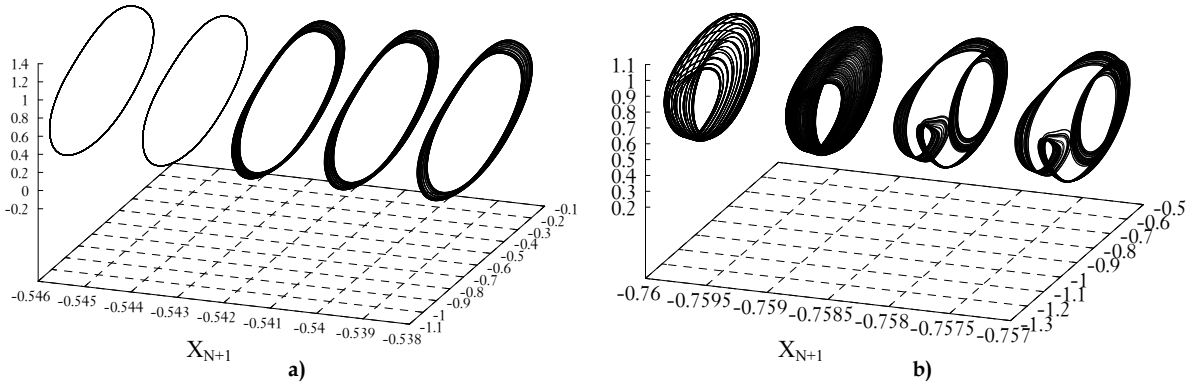

Figure 7. CNN composed by 4 cells and described by the template A= [0.9 1.1 -0.9]. a) System trajectories corresponding to the transition from periodic to quasi-periodic behavior (Naimark-Sacker bifurcation) occurring for $\{X_0; X_{N+1}\}=\{0.66, -0.3665 \ldots -0.361\}$. Initial conditions are assumed to be zero for all cells. b) CNN composed by 4 cells and described by the template A= [0.9 1.1 -0.9]. Torus-to-chaos transition and corresponding trajectories, occurring at $\{X_0; X_{N+1}\}=\{0.66, -0.76\ldots-0.757\}$. Initial conditions are assumed to be zero for all cells.

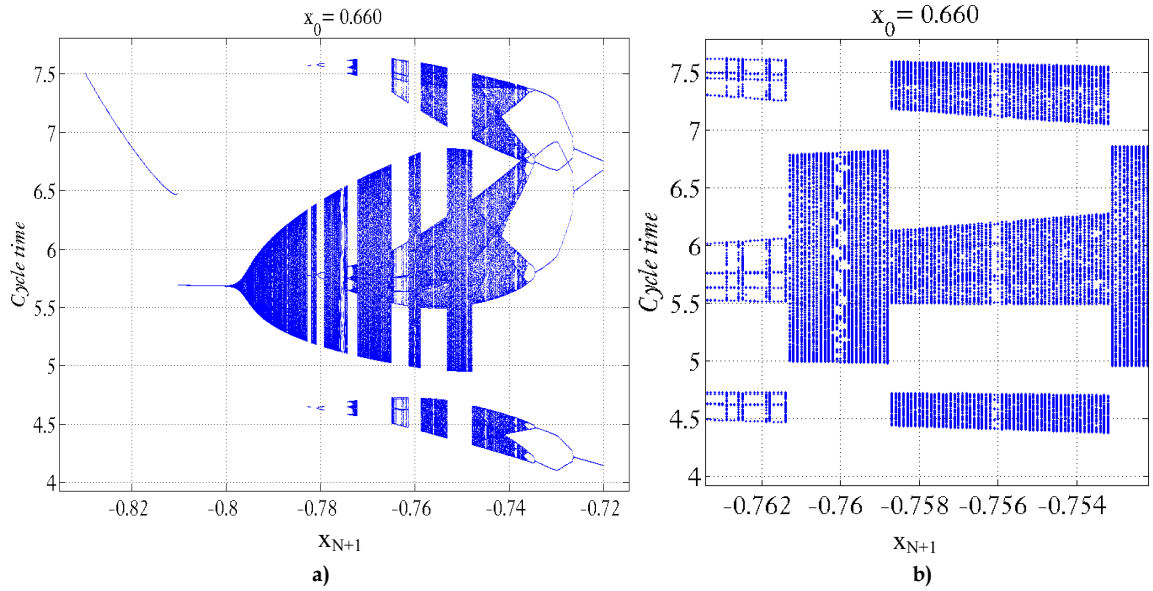

Figure 8. CNN composed by 4 cells and described by the template A= [0.9 1.1 -0.9]. Zoomed representation of an area of Fig. 4, which exhibits multiple transitions among periodic, quasi-periodic and chaotic behavior. Initial conditions are assumed to be zero for all cells. b) Zoomed region of figure a, which exhibits torus-to-chaos transition. Initial conditions are assumed to be zero for all cells.

Fig. 8a represents a region of the bifurcation diagram of Fig. 4, with multiple transitions among periodic, quasi-periodic and chaotic behavior, whereas Fig. 8b zooms on the torus-to-chaos transition; the corresponding trajectories are presented in Fig. 7b. Fig. 9a shows the 2D projection of the Poincare map of a quasi-periodic attractor occurring at $\{X_0, X_{N+1}\}=\{0.66,-0.53\}$ whereas Figs 9b and 9c show the 2D projections of the first return map for the chaotic attractor occurring at $\{X_0, X_{N+1}\}=\{-0.867,-0.463\}$.

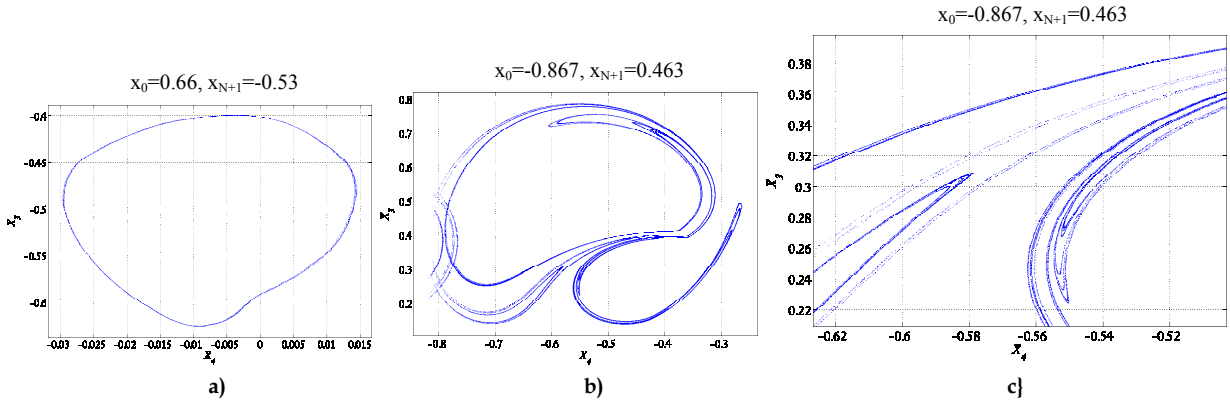

Figure 9. CNN composed by 4 cells and described by the template A= [0.9 1.1 -0.9]. a) 2D projection (on the plane x_3, x_4) of the Poincare map of the quasi-periodic torus attractor occurring at $\{X_0; X_{N+1}\}=\{0.66,-0.53\}$. b) 2D projection (on the plane x_3, x_4) of the Poincare map of the chaotic attractor occurring at $\{X_0; X_{N+1}\}=\{-0.867,-0.463\}$. c) Zoomed part of the map shown in Fig. 14. A fractal structure is observed.

3.2 Coexistence of attractors in 1D CNNs

We will show that the 4-cell CNN, described by the template (6) exhibits the simultaneous existence of different non-stationary attractors.

As pointed out before, the existence of stable equilibrium points does not necessarily exclude the presence of other types of attractors. As shown in Fig. 16, we have found the coexistence of equilibrium points, limit cycles and chaotic attractors, for the following boundary condition parameters:

a) $\{|X_0|s<-(p-1)+s\,,|X_{N+1}+1|s<p-1\}$

b) $\{|X_0+1|s<p-1\,,|X_{N+1}|s<-(p-1)+s\}$

c) $\{|X_0|s<-(p-1)+s\,,|X_{N+1}-1|s<p-1\}$

d) $\{|X_0-1|s<p-1\,,|X_{N+1}|s<-(p-1)+s\}$

The presence of different attractors has also been observed in the unstable region $\{|X_0|<1-(p-1)/s,\ |X_{N+1}|<1-(p-1)/s\}$.

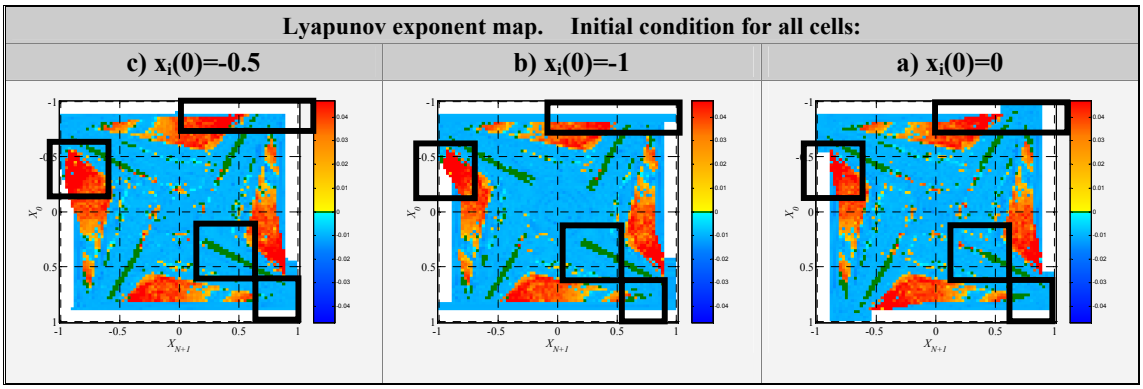

Figure 10. CNN composed by 4 cells and described by the template A= [0.9 1.1 -0.9]. Coexistence of attractors, obtained via different initial conditions: a) $x_i(0)=0$, b) $x_i(0)=-1$, c) $x_i(0)=-0.5$, (i=1..4). Observe the coexistence of chaotic ↔ limit cycle, chaotic ↔ torus and torus ↔ limit cycle attractors.

3.3 Effect of the template parameters on the Lyapunov exponents

Figs. 11 and 12 report the Lyapunov exponents in the boundary condition space (X_0, X_{N+1}), obtained by varying the parameters s and p of the template (6).

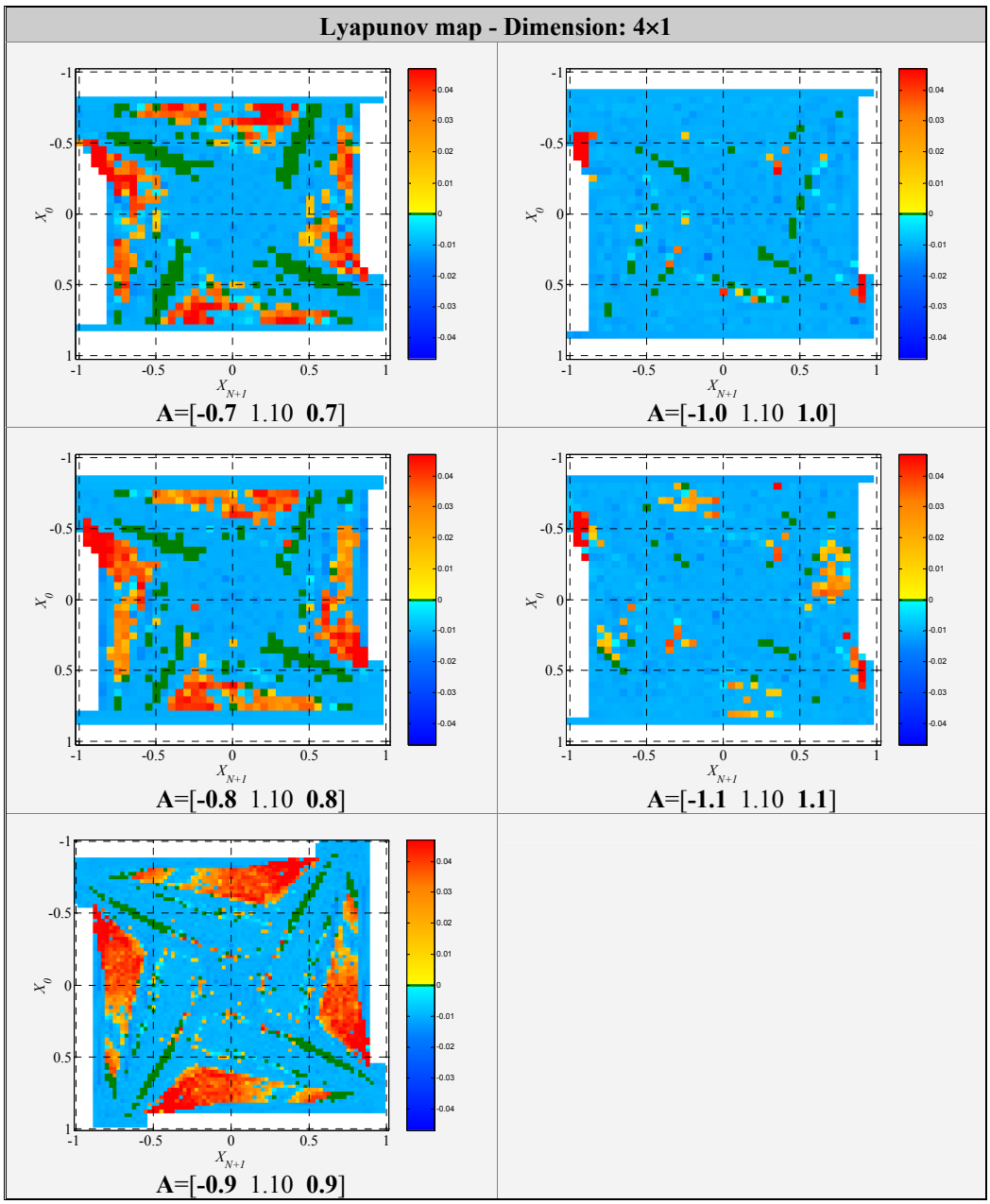

Figure 11. CNN composed by 4 cells and described by template (6). Lyapunov exponent maps, obtained by varying the parameter s in the template (6). The initial conditions have been set to -1, for all cells.

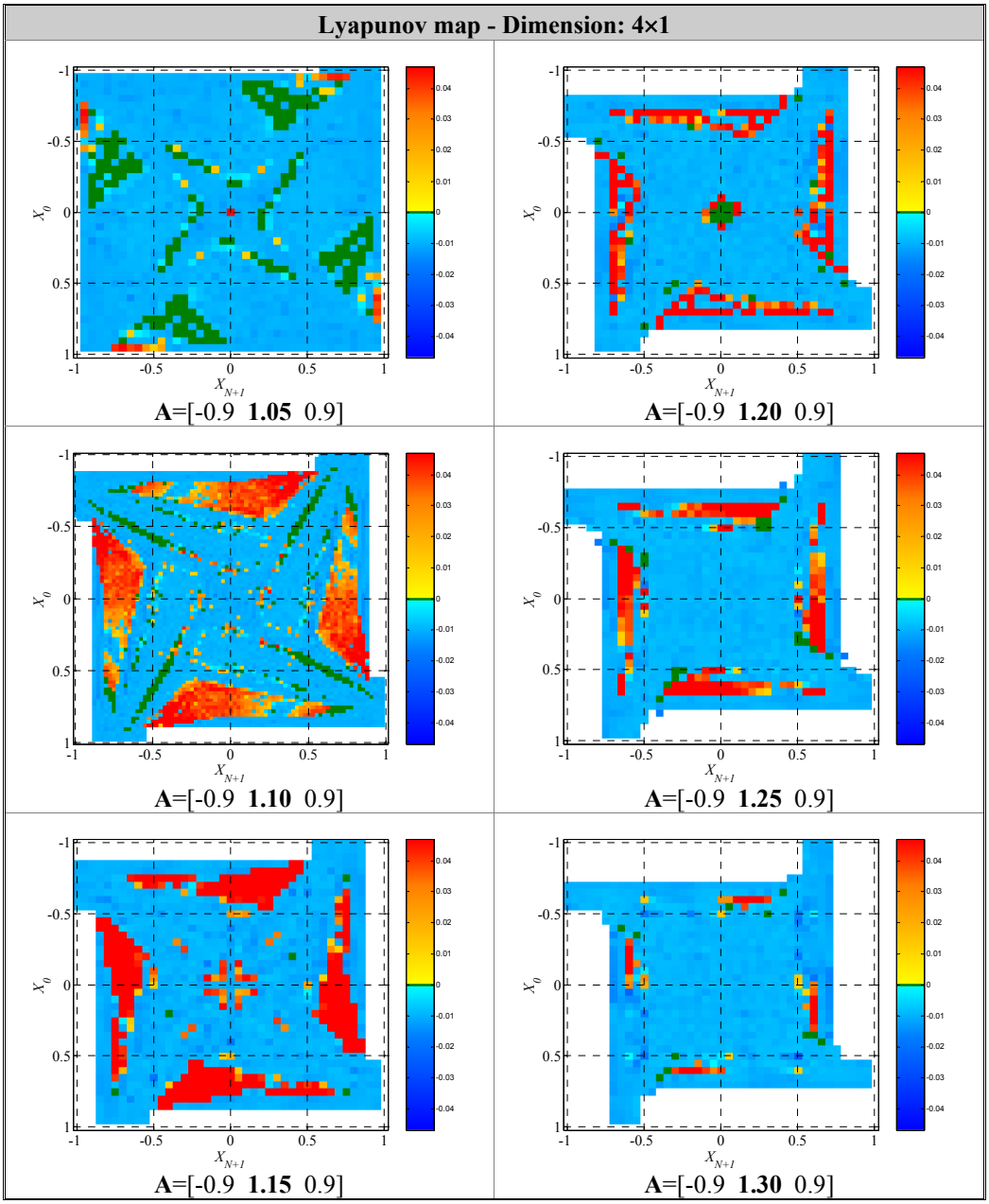

Figure 12. CNN composed by 4 cells and described by template (6). Lyapunov exponent maps, obtained by varying the parameter p in the template (6). The initial conditions are assumed to be zero for all cells.

3.4 Complex dynamics and hyperchaos in higher dimensional CNNs

Fig. 13 shows the influence of the number of cells on the network dynamics. It is observed that the Lyapunov maps of CNNs with a even number of cells present significant similarities. Fig 14 evidences hyperchaotic behavior (more than one positive Lyapunov exponents) in CNNs composed by 6, 7 and 8 cells.

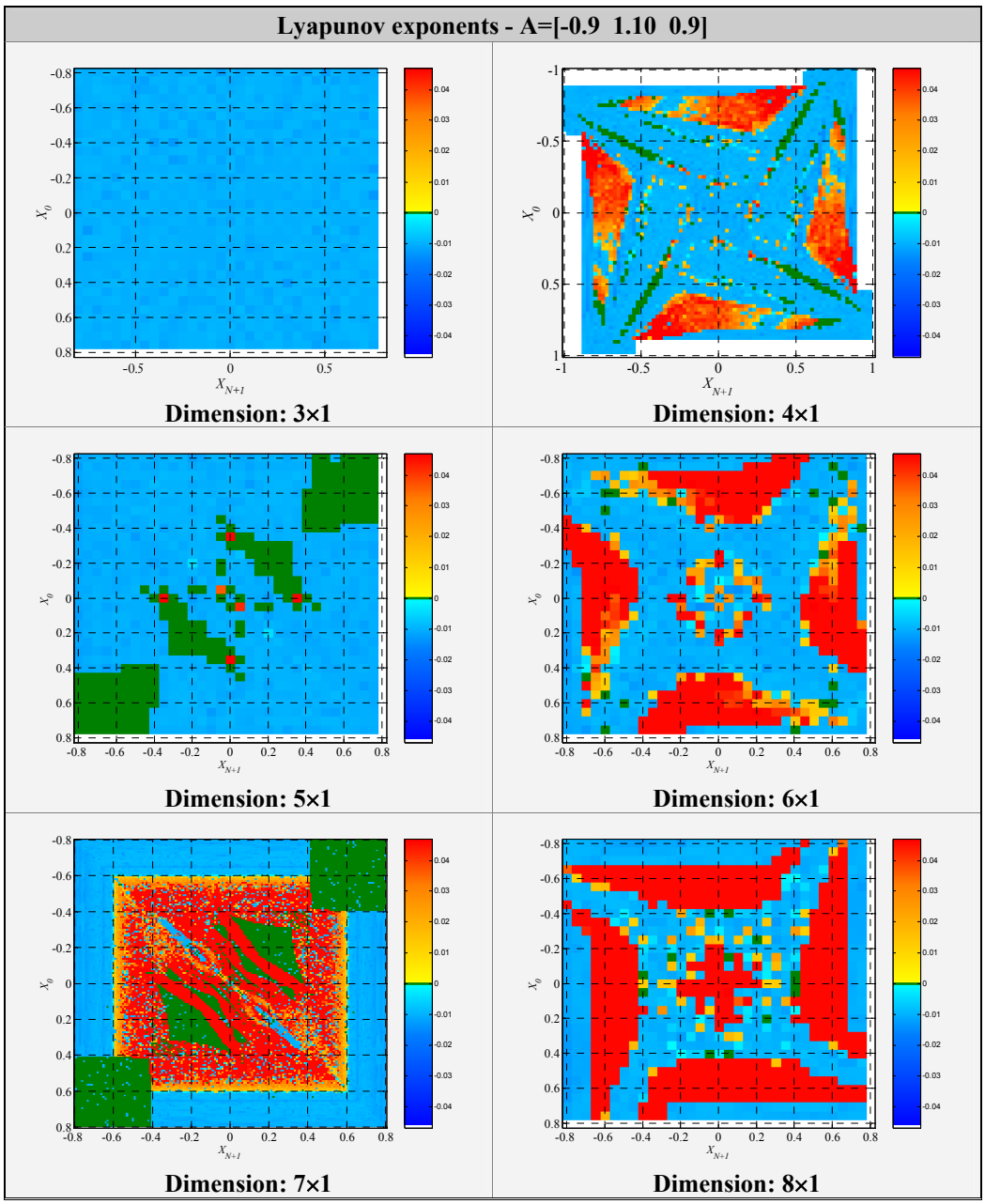

Figure 13. CNN described by the template A= [0.9 1.1 -0.9]. Influence of the CNN dimension on the Lyapunov map. The initial conditions are assumed to be zero for all cells.

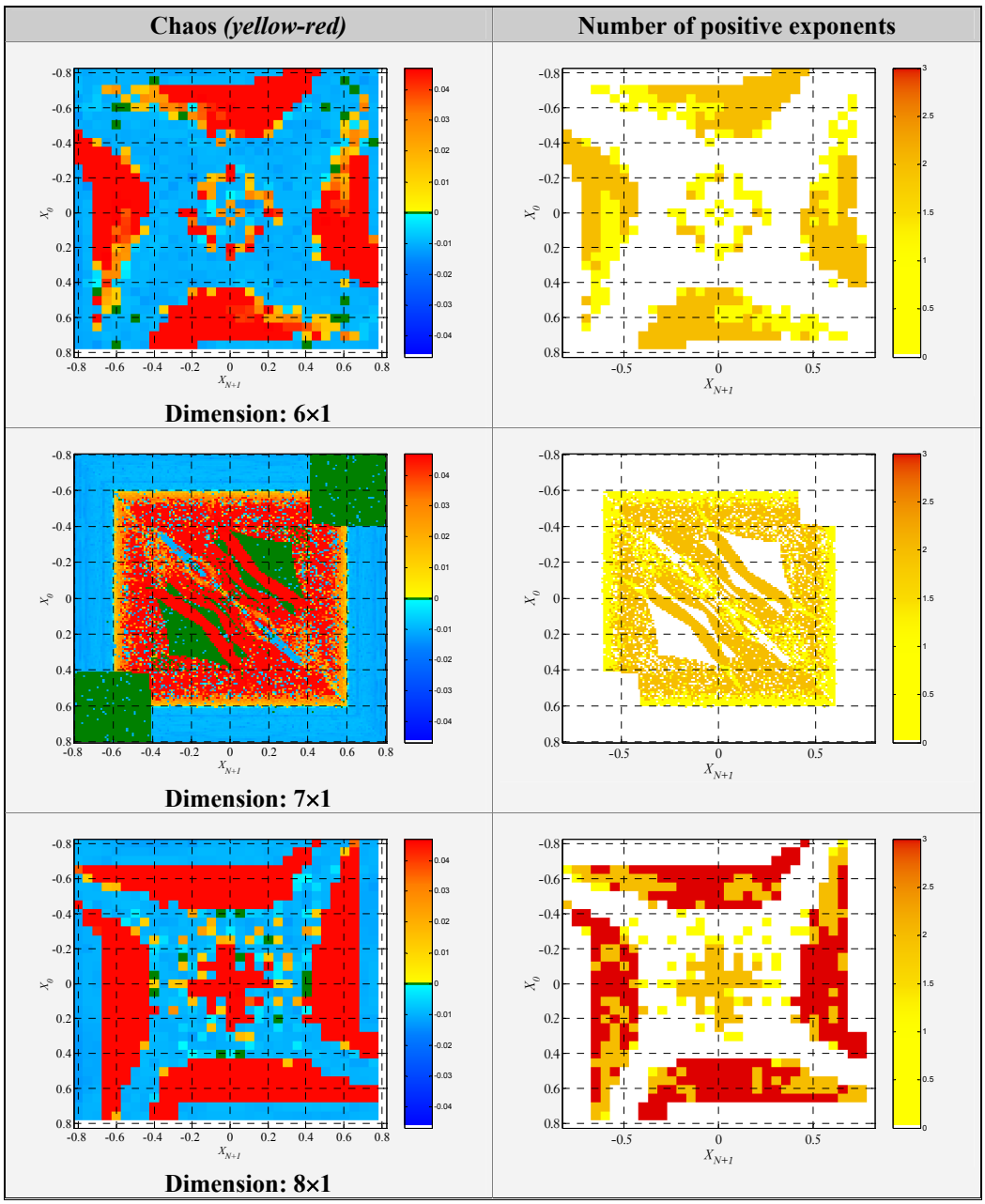

Figure 14. CNN described by the template A= [0.9 1.1 -0.9]. Hyperchaos has been observed in 6x1 , 7×1 and 8×1 CNNs. The number of positive Lyapunov exponents are reported in the right column, through a color code. The initial conditions are assumed to be zero for all cells.

4. Conclusions

We have investigated the effect of constant boundary conditions of CNN global dynamic behavior. As a case study we have considered CNNs described by one-dimensional templates. By exploiting the results presented in [4] and [12], we have proved that if the off-diagonal elements have the same sign, the CNN is completely stable for any external constant inputs and/or boundary conditions. Then we have shown that in a CNN described by an opposite-sign template, the boundary conditions behave as bifurcation parameters and can give rise to a rather complex dynamic behavior. In particular, through the numerical computation of the Lyapunov exponents, we have observed the occurrence of periodic, quasi periodic and chaotic attractors and we have investigated the bifurcation processes that determine the transition from qualitatively different behaviors.

We have also shown that simple 1D CNNs may exhibit the coexistence of several non-stationary attractors and that hyperchaotic behavior (i.e. more than one positive Lyapunov exponents) may occur in CNNs composed by more than five cells.
The results presented in the paper may open the possibility of exploiting constant boundary conditions and constant external inputs for designing new CNN functionalities.

5. References

[1] L. O. Chua and L. Yang, "Cellular neural networks: theory", *IEEE Transactions on Circuits and Systems I*, vol. 35, pp. 1257-1272, Oct. 1988.

[2] C. W. Wu and L. O. Chua, "A more rigorous proof of complete stability of cellular neural networks", *IEEE Transactions on Circuits and Systems I*, Vol. 44, no. 4, pp. 370-371, 1997.

[3] L. O. Chua and C. W. Wu, "The universe of stable CNN templates," *International Journal of Circuit Theory and Applications*, vol. 20, pp. 497-517, 1992.

[4] M. Gilli, "Stability of cellular neural networks and delayed cellular neural networks with nonpositive templates and nonmonotonic output functions," *IEEE Transactions. on Circuits and Systems I,* pp. 518-528, vol. 41, 1994

[5] N.Takahashi and L.O.Chua, "On the complete stability of nonsymmetric cellular neural networks", *IEEE Transactions on Circuits and Systems I*, vol.45, no.7, pp.754-758, July 1998.

[6] L. O . Chua and T. Roska, "Stability of a class of nonreciprocal cellular neural networks", *IEEE Transactions. on Circuits and Systems I*, Vol. 37, No. 12, pp. 1520-1527, 1990.

[7] F. Zou and J. A. Nossek, "Stability of cellular neural networks with opposite-sign templates," *IEEE Transactions on Circuits and Systems.* I, vol. 38, pp. 675–677, 1991.

[8] G. De Sandre, "Stability of 1-D-CNN's with Dirichlet boundary conditions and global propagation dynamics," *IEEE Transactions on Circuits and Systems I,* vol. 47, pp. 785-792, 2000.

[9] P. Thiran, G. Setti, and M. Hasler, "An approach to information propagation in 1-D cellular neural networks - Part I: local diffusion" *IEEE Transactions on Circuits and Systems I*, vol. 45, no. 8, pp. 777-789, 1998.

[10] G. Setti, P. Thiran, and M. Hasler, "An approach to information propagation in 1-D cellular neural networks - Part II: global propagation" *IEEE Transactions on Circuits and Systems I*, vol. 45, no. 8, pp. 790-811, 1998.

[11] M. Biey, P. Checco, and M. Gilli, "Bifurcation and chaos in CNNs", *Journal of Circuits Systems and Computers*, vol. 12, no. 4, pp. 417-433, August 2003.

[12] F. Zou and J. A. Nossek, "Bifurcation and chaos in cellular neural networks," *IEEE Transactions on Circuits and Systems I,* vol. 40, pp. 166–173, Mar. 1993.

[13] M. Biey, M. Gilli, P. Checco, "Complex dynamic phenomena in space-invariant cellular neural networks", *IEEE Transactions on Circuits and Systems I,* Volume: 49 Issue: 3 , March 2002 pp. 340 -345.

[14] G. Manganaro, P. Arena, L. Fortuna "Cellular neural networks: chaos, complexity and VLSI processing", Springer Verlag, New York; ISBN: 3540652027, 1999

[15] T. Roska and A. Rodríguez-Vázquez (editor), "Towards the visual microprocessor: VLSI design and the use of cellular network universal machines", John Wiley & Sons; ISBN: 0471956066, 2000.

[16] The ALADDIN System, http://www.analogic-computers.com/

[17] P. P. Civalleri and M. Gilli, "Global dynamic behaviour of a three cell connected component detector CNN," *International Journal of Circuit Theory and Applications*, vol. 23, no. 2, pp. 117-135, March 1995.

[18] N. Takahashi and T. Nishi, "On the global stability of two-cell cellular neural networks with opposite-sign connections," *Proceedings of the 15th European Conference on Circuit Theory and Design*, vol. 3, pp.93-96, August 2001.

[19] P. P. Civalleri and M. Gilli, "A Spectral Approach to the Study of Propagation Phenomena in CNNs", *Int. J. Circuit Theory and Applications*, vol. 24, 1996, pp. 37-48.

[20] M. Gilli,"Analysis of periodic oscillations in finite-dimensional CNNs through a spatio-temporal harmonic balance technique," *Int. J. Circuit Theory and Applications*, vol. 25, pp. 279-288, July-August 1997.

[21] M. Di Marco, A. Tesi and M. Forti, "Bifurcations and oscillatory behaviour in a class of competitive Cellular Neural Networks," *Int. Journal of Bifurcation and Chaos*, Vol. 10, pp. 1267-1293, 2000

[22] M. Di Marco, M. Forti and A. Tesi, "Existence and characterization of limit cycles in nearly symmetric neural networks", *IEEE Transactions on Circuits and Systems I*, vol .49, no. 8, pp. 979-992, 2002

[23] M. Di Marco, M. Forti and A. Tesi, "Complex dynamics in nearly symmetric three-cell cellular neural networks", *Int. Journal of Bifurcation and Chaos*, vol. 12, no. 6, pp. 1357-1362, 2002

[24] Zou, F. & Nossek, J. A. "A chaotic attractor with cellular neural networks" *IEEE Transactions on Circuits and Systems I,* vol. 38, 811-812, 1991.

[25] M. Gilli, "Strange attractors in delayed cellular neural networks," *IEEE, Transactions on Circuits and Systems I*, pp. 849- 853, vol. 40, 1993.

[26] I. Petrás, Tamás Roska, and Leon O. Chua "New spatial-temporal patterns and the first programmable on-chip bifurcation test-bed" *IEEE Transactions. on Circuits and Systems I,* pp. 619-633, vol. 51, May 2003

[27] P. Thiran, "Influence of boundary conditions on the behavior of cellular neural networks," *IEEE Trans. on Circuits and Systems I,* vol. 40, 1993

[28] I. Petrás, P. Checco, M. Gilli, M. Biey, and T. Roska, "On the effect of boundary conditions on CNN dynamics: stability and instability; bifurcation processes and chaotic phenomena", *Proceedings. of ISCAS 2003*, pp. 590-593, vol. III, 2003

[29] J.P. Eckmann and D. Ruelle, "Ergodic Theory of Chaos and Strange Attractors", *Review of Modern Physics*, vol. 57, pp. 617-659, 1985.